

# Human Absorbed Dose Estimation of $^{89}\text{Zr}$ -Anti-HER2 Complex Based on Animal Data

Samaneh Zolghadri<sup>1</sup>, Arezou Karimian<sup>1</sup>, Hassan Yousefnia<sup>1\*</sup>

1. Radiation Application Research School, Nuclear Science and Technology Research Institute (NSTRI), Tehran, 14155-1339, Iran.

ARTICLE INFO	ABSTRACT
<b>Article type:</b> Original Paper	<b>Introduction:</b> This study aimed to estimate the radiation absorbed dose of human organs after injection of a high-potential PET radioimmunoconjugate of HER2+ breast cancers using the medical internal radiation dose (MIRD) method and the radiation dose assessment resource (RADAR) formalism.
<b>Article history:</b> Received: Feb 28, 2024 Accepted: Aug 21, 2024	<b>Material and Methods:</b> $^{89}\text{Zr}$ was produced by the nuclear reaction of $^{89}\text{Y}$ with protons (p,n), and purified by a column filled with ZR resin. The radionuclide, chemical, and radiochemical purities of the $^{89}\text{Zr}$ solution were measured using gamma spectrometry, inductively coupled plasma (ICP), and radio-thin-layer chromatography (RTLC) methods, respectively. The conjugated anti-HER2 with deferoxamine (DFO) was labeled with an in-house produced $^{89}\text{Zr}$ at the optimized condition to prepare $^{89}\text{Zr}$ -Anti-HER2, and its radiochemical purity was assessed by the RTLC method. The stability of the radioimmunoconjugate was assessed in Phosphate-buffered saline (PBS) buffer and human serum at various intervals. Biodistribution of the final complex was studied in tumor-bearing mice at specified intervals. Finally, the absorbed dose of human organs was estimated using the MIRD method and RADAR formalism based on animal data.
<b>Keywords:</b> Zirconium-89 Positron-Emission Tomography Breast Neoplasms Radiation	<b>Results:</b> $^{89}\text{Zr}$ radionuclide was produced by the radiochemical and radionuclide purities of >99%, and >99.99%, respectively, while the chemical impurities were < 0.1 ppm. The radiolabeled antibody was prepared with radiochemical purity >98% at optimized conditions. The results showed the liver received the maximum amount of the absorbed dose of 1.49 mGy/MBq, and other organs received < 0.87 mGy/MBq. <b>Conclusion:</b> $^{89}\text{Zr}$ -Anti-HER2 complex is a promising agent for PET imaging of patients with HER2+ tumors with high safety in the country.

► Please cite this article as:

Zolghadri S, Karimian A, Yousefnia H. Human Absorbed Dose Estimation of  $^{89}\text{Zr}$ -Anti-HER2 Complex Based on Animal Data. Iran J Med Phys 2025; 22: 203-208. 10.22038/ijmp.2025.78414.2386.

## Introduction

Although the Coronavirus Disease 2019 (COVID-19) has posed significant challenges to the diagnosis and treatment of cancer, cancer remains a major public health concern worldwide. Breast cancer is one of the causes of death in women and has shown an increasing trend in recent years [1]. Among the standard diagnostic methods for breast cancers, including magnetic resonance imaging (MRI), mammography, computerized tomography (CT), ultrasound, biopsy, and positron emission tomography (PET) [2], the latter is an interesting tool that can detect tumor cells at the molecular level with high quality due to its ultra-high sensitivity [3,4].

Monoclonal antibodies (mAbs) have been very effective in cancer treatment and are being developed nowadays. mAbs have tumor-specific antigens; this feature helps to deliver drugs to cancer cells and causes the most minor damage in normal cells. Trastuzumab is one of the common mAbs that has good toxicity in breast cancer cells by its binding to the human epidermal growth factor receptor 2 (HER2) [5]. HER2 is overexpressed in 20–30% of breast cancer tumors, a subtype commonly referred to as HER2-positive breast cancer [6].

However, PET is a powerful technique for molecular imaging; the most common PET radionuclides, including  $^{11}\text{C}$  ( $t_{1/2}=20.4$  min),  $^{15}\text{O}$  ( $t_{1/2}=2.1$  min),  $^{13}\text{N}$  ( $t_{1/2}=10$  min), and  $^{18}\text{F}$  ( $t_{1/2}=109.8$  min), have short half-life to match the biological half-life of the mAbs [7]. Recently, two new PET radionuclides,  $^{123}\text{I}$  and  $^{89}\text{Zr}$ , have been introduced as high-potential radionuclides for developing tracers with longer pharmacokinetics and slowly accumulating targeting vectors.  $^{89}\text{Zr}$  possesses unique physical and chemical characteristics, such as a 78.41-h half-life, 76.6% electron capture, 22.3% positron emission with a maximum energy of 897 keV (mean 397 keV, average range 1.18 mm), and a strong gamma emission at 908.9 keV (100% intensity), making it a promising candidate for the development of monoclonal antibody (mAb)-based radiopharmaceuticals [8].

Radiation absorbed dose, defined as the energy deposited in human organs by ionizing radiation, is a crucial parameter for assessing the risks associated with the administration of new radiopharmaceuticals and determining the maximum allowable administered activity of the radiotracer [9,10]. On the

\*Corresponding Author: Tel: +98-2188221103; Email: hyousefnia@aeoi.org.ir

other hand, a lower administered activity can reduce the signal-to-noise ratio (SNR) in the imaging process, potentially compromising image quality. Also, the absorbed dose of the critical organs should be kept as low as possible. Currently, in nuclear medicine, the MIRD method is widely used for internal dose calculations [11,12], with the RADAR resource being one of the most advanced tools for these computations [13].

Due to the high potential of  $^{89}\text{Zr}$  Zr-DFO-Trastuzumab for PET imaging of HER2+ tumors, this study aimed to estimate the human organ absorbed dose of this radiolabeled compound based on the animal data. For this purpose, the radioimmunoconjugate was prepared under optimized conditions, and the radiochemical purity of the radiolabeled compound was assessed using the RTLC method. After stability assessment of  $^{89}\text{Zr}$  Zr-Anti-HER2 complex in PBS and human serum, the biodistribution of the radiolabeled complex was assessed in tumor-bearing nude mice at different intervals. The absorbed dose of human organs was estimated using MIRD and Spark et al. [14] methods.

## Materials and Methods

Trastuzumab mAb was purchased from Ariogen Pharmed Co. (Iran). The DFO chelator and ZR resin were obtained from Macrocyclic Inc. (USA) and TrisKem International Co. (France), respectively. All other chemicals and reagents were purchased from Sigma Aldrich Co. Nude mice were acquired from Royan Institute, Iran. A Bio-scan AR-2000 radio TLC scanner instrument (Bio-scan, Paris, France) was used for radiochemical purity assessment. A p-type coaxial high-purity germanium (HPGe) detector (model: NIGC-4020) was utilized to measure radionuclidic purity. Student's T-test was used to compare the biodistribution data with a statistical significance of  $P < 0.05$ . This study was approved by the NSTRI Ethical Committee (Approval No.: PRC-B5-98-001).

### Production and Quality Control of $^{89}\text{Zr}$

$^{89}\text{Zr}$  was produced in a 30 MeV cyclotron (Cyclone-30, IBA) by  $^{89}\text{Y}(p,n)^{89}\text{Zr}$  nuclear reaction according to the previously published procedure [15]. Briefly, the  $^{89}\text{Y}_2\text{O}_3$  pellet target (330 mg) was irradiated with 14 MeV proton energy (25  $\mu\text{A}$ ; 5 h). The dissolved target in 6 M HCl was passed through a preconditioned column filled with ZR resin (200 mg) to separate the target and other possible impurities from the  $^{89}\text{Zr}$ . In this step, the column was washed 4 times with 2.5 mL HCl (6 M) solution and 4 times with 2.5 mL water. Finally, the column was washed with 1.0 M oxalic acid solution (1.5 mL) to obtain  $^{89}\text{Zr}$  in oxalic form. The chemical, radiochemical, and radionuclide purities of the final solution were determined using Inductively Coupled Plasma Mass Spectrometry (ICP-MS), RTLC, and gamma spectrometry, respectively.

### Preparation and Quality Control of $^{89}\text{Zr}$ Zr-Anti-HER2 Complex

The preparation of the radiolabeled compound was carried out using another published method [8]. A measured amount of  $^{89}\text{Zr}$  Zr-oxalic acid (37 MBq) was combined with 2 M  $\text{Na}_2\text{CO}_3$  in a 10-mL borosilicate vial. The vial was shaken thoroughly, followed by the addition of 0.5–2 mg of DFO-Trastuzumab and HEPES buffer (4-(2-hydroxyethyl)-1-piperazineethanesulfonic acid). The reaction proceeded for one hour, after which the resulting complex was used for subsequent steps. The radiochemical purity of the final radiolabeled complex was assessed using the RTLC method, employing Whatman paper and a 20 mM citric acid solution (pH 4.5).

### Stability studies of the radioimmunoconjugate

The stability of the radiolabeled compound was evaluated in Phosphate-buffered saline (PBS) buffer at 4°C and freshly prepared human serum at 37°C. The radiochemical purity of the radiolabeled compound was assessed using the RTLC method at various time intervals, including 2-, 4-, 24-, and 48-hours post-incubation.

### Biodistribution of the final complex in tumor-bearing mice

Approximately three million BT474 cells were subcutaneously injected into the 4-8 weeks-old nude mice weighing 20-25 g. The biodistribution of the final radiolabeled compound was studied in the HER2+ tumor-bearing mice, after the tumors had grown. The mice were sacrificed at specified intervals, and the radioactivity of each organ was measured based on the energy peak of the 908.9 keV gamma ray, as outlined in (equation 1) [16].

$$A = \frac{N}{\varepsilon \gamma t_s k_1 k_2 k_3 k_4 k_5} \quad (1)$$

In this context,  $\varepsilon$  denotes the absolute detection efficiency corresponding to the energy of the photopeak, whereas  $\gamma$  represents the probability of gamma-ray emission at that specific energy level. The variable  $t_s$  indicates the spectrum's live counting time in seconds, and  $m$  refers to the measured sample's mass in kilograms. Correction coefficients  $k_1$  through  $k_5$  are introduced to compensate for: (1) decay occurring between sample collection and the beginning of the measurement, (2) decay throughout the acquisition period, (3) self-attenuation of photons within the sample matrix, (4) loss of pulse signals due to random summing, and (5) coincidence effects. Finally,  $N$  stands for the net peak area after applying all relevant corrections.

$$N = N_s - \frac{t_s}{t_b} N_b \quad (2)$$

Here,  $N_s$  designates the net photopeak area observed in the sample spectrum, while  $N_b$  represents the corresponding net area obtained from the background spectrum. The variable  $t_s$  refers to the live

acquisition time of the background spectrum, measured in seconds [17].

To assess the radiotracer uptake in various tissues, the percentage of injected dose per gram (%ID/g) was calculated by dividing the measured activity in each organ (A) by the total injected activity (uncorrected for decay), and then normalizing the result by the tissue weight. Data are presented as mean  $\pm$  standard deviation, and group comparisons were performed using the Student's t-test for statistical significance [17,18].

$$\% \text{ID} = \frac{A}{\text{injected activity} \times \text{Tissue weight}_{(\text{g})}} \times 100 \quad (3)$$

#### Estimation of Accumulated Activity in Human Organs

To estimate the accumulated activity in target organs, the percentage of the injected dose per gram (%ID/g), without correction for radioactive decay, was plotted as a function of time. The calculation followed the formulation described in Equation 4, where A(t) indicates the measured activity in the organ at a specific time t.

$$\tilde{A} = \int_0^\infty A(t) dt \quad (4)$$

In calculating the area under the time–activity curve (AUC), linear interpolation was applied between consecutive experimental data points. To estimate the tail of the curve, the last data point for each source organ was extrapolated to infinity using a mono-exponential decay model, with the decay constant set equal to the physical decay rate of  $^{89}\text{Zr}$ .

For extrapolating accumulated activity from animal models to humans, the approach based on relative organ mass scaling, originally proposed by Sparks et al. (Equation 5) [15], was utilized. This method employed standard reference values for human organ masses [19] to perform the conversion.

$$\tilde{A}_{\text{Human organ}} = \tilde{A}_{\text{Animal organ}} \times \frac{\text{Organ mass}_{\text{human}} / \text{Body mass}_{\text{human}}}{\text{Organ mass}_{\text{animal}} / \text{Body mass}_{\text{animal}}} \quad (5)$$

#### Equivalent absorbed dose calculation

RADAR formalism was utilized for the calculation of the absorbed dose in human organs (Equation 6) [13]:

$$D = \tilde{A} \times \text{DF} \quad (6)$$

Where DFs are the constant dose factors, which are available in the OLINDA/EXM software [20].

## Results

### Production and quality control of $^{89}\text{Zr}$

$^{89}\text{Zr}$  was produced as zirconium oxalate after the bombardment of a  $^{89}\text{Y}_2\text{O}_3$  pellet target in a 30 MeV cyclotron, and washing the column with oxalic acid. The gamma spectrometry of the final solution using a HPGe detector demonstrated two major gamma rays originating from  $^{89}\text{Zr}$ . The radiochemical purity evaluation of the produced radionuclide showed a radiochemical purity higher than 99%. The chemical purity assessment of the final solution, determined by the Inductively Coupled Plasma Optical Emission Spectrometry (ICP-OES) method, demonstrated the total impurity of less than 0.1 ppm for the metal ions.

### Preparation and quality control of [ $^{89}\text{Zr}$ ]Zr-Anti-HER2 complex

[ $^{89}\text{Zr}$ ]Zr-Anti-HER2 complex was prepared at optimized conditions, where the chelator: mAb ratio was 10:1, the  $^{89}\text{Zr}$ : mAb ratio was 74 MBq:1 mg, and the reaction temperature was 37°C, and the reaction pH was 7. The radiochemical purity of the complex, evaluated by the RTLC method 1 h post-incubation, showed a radiochemical purity greater than 98%.

### Stability studies of the radioimmunoconjugate

The radiochemical purity assessment of the final radiolabeled compound after incubation in PBS buffer (4°C) and human serum (37°C) showed the complex is a purity of more than 97% even after 48 h post-incubation.

### Biodistribution of [ $^{89}\text{Zr}$ ]Zr-Anti-HER2 complex in tumor-bearing mice

The biodistribution of the final prepared complex was evaluated in tumor-bearing nude mice. Non-decay corrected curves after injection of the [ $^{89}\text{Zr}$ ] Zr-Anti-HER2 complex are shown in Figure 1.

### Calculation of accumulated activity in human organs

The equivalent absorbed dose in each human organ after injection of the final complex is demonstrated in Figure 2.

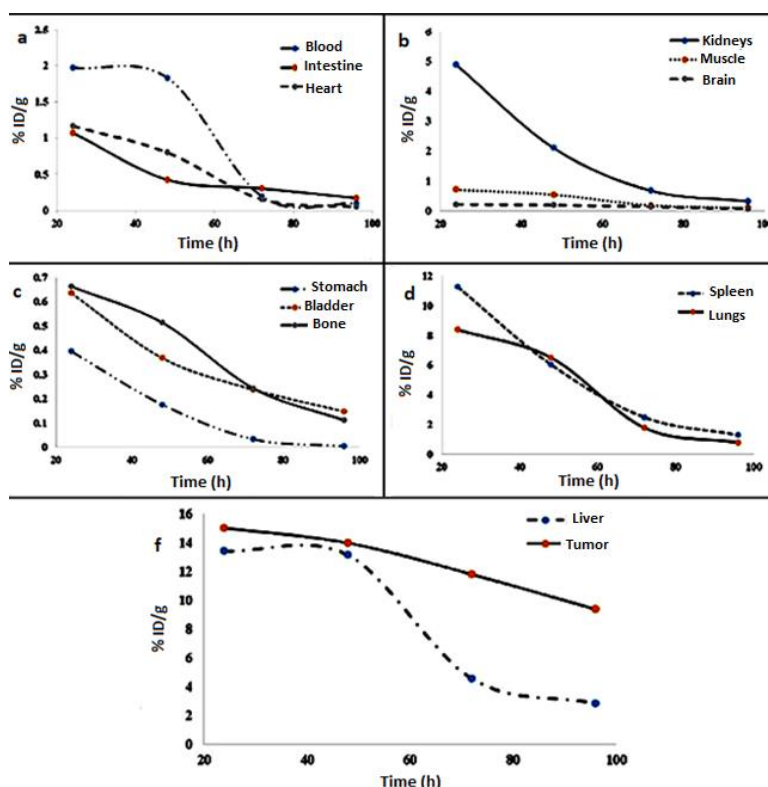


Figure 1. Non-decay corrected curves after injection of the  $^{89}\text{Zr}$ -Anti-HER2 complex in (a) blood, intestine, and heart; The curve shows the activity removed from the blood slowly; (b) kidneys, muscle, and brain; The kidneys exhibit the high initial uptake, followed by a gradual decrease; In contrast, the muscle and brain show very low and relatively stable uptake; (c) stomach, bladder, and bone; (d) spleen and lungs; Both tissues demonstrate a gradual decrease in concentration; (e) liver and tumor; The liver demonstrates the high initial uptake, which significantly decreases over time; In contrast, the tumor exhibits a lower but more sustained concentration, indicating selective targeting of the tumor.

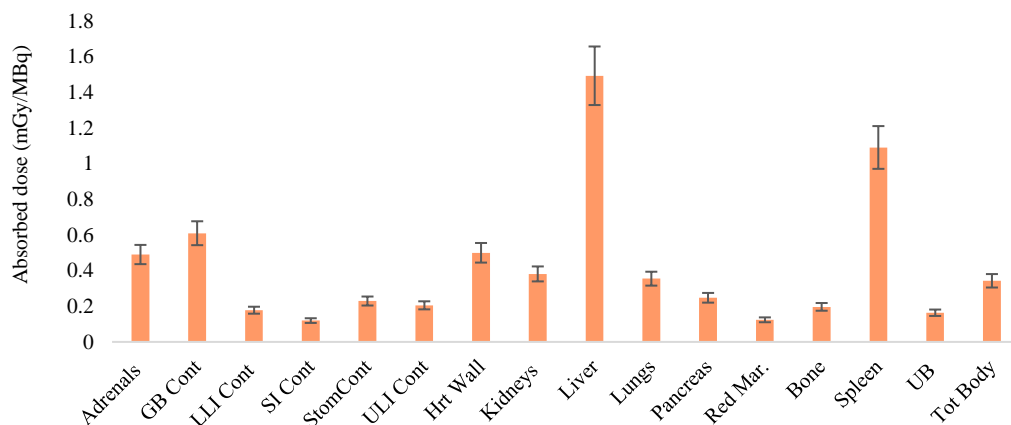


Figure 2. Equivalent absorbed dose in each human organ after injection of the  $^{89}\text{Zr}$ -Anti-HER2 complex

## Discussion

Breast cancer is one of the most prevalent cancers worldwide, and HER2+ breast cancer accounts for a high percentage of these cases [6].  $^{89}\text{Zr}$  is one of the emerging PET radionuclides, characterized by unique physical and chemical properties, making it suitable for use in new PET radiopharmaceuticals with slow pharmacokinetics, such as monoclonal antibody-based agents, to enable imaging at longer time intervals. The production of  $^{89}\text{Zr}$  to develop new radiopharmaceuticals

for radioimmunoPET applications has recently been reported in the country [15]. Also, due to the high potential of  $^{89}\text{Zr}$ -Trastuzumab to detect HER2+ tumors of the patients in clinical trials [21,22], this valuable agent was accordingly developed in the country [8].

The novelty of the study lies in the development of the  $^{89}\text{Zr}$ -labeled radioimmunoconjugate for PET imaging of HER2+ breast cancers, utilizing the longer half-life of  $^{89}\text{Zr}$  to match the slow pharmacokinetics of monoclonal antibodies.



Table 1. The comparison of absorbed dose in different organs with the other  $^{89}\text{Zr}$ -anti-HER2 complex

Target Organ	Absorbed dose (mGy/MBq)		
Adrenals	0.57	0.80	0.49
Stomach	0.43	0.63	0.23
Heart Wall	1.11	1.12	0.50
Kidneys	0.90	1.23	0.38
Liver	1.32	1.63	1.49
Lungs	0.81	0.59	0.35
Pancreas	0.56	0.78	0.25
Bone	0.50	0.79	0.19
Red Marrow	0.45	0.69	0.12
Spleen	1.09	0.80	0.86
Urinary Bladder	0.33	0.42	0.16
Total Body	0.37	0.55	0.34
Reference	[21]	[22]	This study

The in-house production of  $^{89}\text{Zr}$  with high RCP, combined with the optimized labeling of Trastuzumab, demonstrates the potential of a promising new radiopharmaceutical for enhanced targeted cancer imaging. The innovative application of the MIRDOSE method and RADAR formalism to estimate human organ absorbed doses based on animal data ensures the compound's safety, while stability and biodistribution assessments further validate its potential for clinical use. This work represents a significant advancement in personalized cancer diagnostics, leveraging new radionuclides and radiopharmaceuticals.

Utilizing preclinical animal data to estimate absorbed doses in humans is a well-established and commonly adopted strategy in the early phases of radiopharmaceutical development. This methodology is recognized as a critical prerequisite and aligns closely with the recommendations provided in International Commission on Radiological Protection (ICRP) Publication 62 [23,24].

Following this standard approach, the current study was conducted to evaluate organ-specific absorbed doses in humans for the novel [ $^{89}\text{Zr}$ ]Zr-Anti-HER2 complex, which was prepared using locally produced  $^{89}\text{Zr}$ . The objective was to facilitate the potential clinical implementation of this radiotracer in PET imaging for patients with HER2-positive malignancies in the country.

[ $^{89}\text{Zr}$ ]Zr-Anti-HER2 complex was prepared at optimized conditions with radiochemical purity > 98%. The human absorbed dose of the complex, based on animal data, showed the liver received the largest amount of the absorbed dose with  $1.49 \pm 0.13$  mGy/MBq, after injection of the complex. The estimated absorbed dose to human organs in this study was compared with similar studies conducted in humans (Table 1).

The comparison of the human organ absorbed dose with the amounts from the trials showed the same trends for the absorbed dose. The liver receives the highest absorbed dose of 1.49 mGy/MBq after injection of  $^{89}\text{Zr}$ -DFO-Trastuzumab, and the result is comparable with other similar  $^{89}\text{Zr}$ -based radiolabeled mAbs, including

$^{89}\text{Zr}$ -DFO-Bevacizumab [25], and  $^{89}\text{Zr}$ -DFO-Cetuximab [26], which receive the maximum absorbed doses of 1.12 and 0.94 mGy/MBq, respectively. However, there are differences in the amounts of absorbed dose in all studies due to the different pharmacokinetics of the radiotracer in humans and animals. Additionally, the absorbed dose values are highly comparable for certain organs, including the adrenals, spleen, and total body.

## Conclusion

This study estimated the human organ absorbed dose of the [ $^{89}\text{Zr}$ ]Zr-Anti-HER2 complex, a promising radioimmunoconjugate for detecting HER2+ breast cancer using PET imaging. The complex was produced using in-house  $^{89}\text{Zr}$  and demonstrated high radiochemical purity (>98%). The liver was found to receive the highest absorbed dose ( $1.49 \pm 0.13$  mGy/MBq), while other organs received significantly lower doses. These results suggest that the [ $^{89}\text{Zr}$ ] Zr-Anti-HER2 complex is a safe and effective agent for further clinical use in detecting HER2+ tumors.

## Acknowledgment

The authors would like to acknowledge the invaluable scientific and financial support of the International Atomic Energy Agency (IAEA) for this research under the Coordinated Research Project (Project Code: F22071, IAEA Research Contract No: 23763).

## References

1. Siegel RL, Miller KD, Wagle NS, Jemal A. Cancer statistics. *Ca Cancer J Clin*. 2023 Jan 1;73(1):17-48.
2. Wang L. Early diagnosis of breast cancer. *J Sens*. 2017 Jul 5;17(7):1572.
3. Wu Y, Fu F, Meng N, Wang Z, Li X, Bai Y, et al. The role of dynamic, static, and delayed total-body PET imaging in the detection and differential diagnosis of oncological lesions. *Cancer Imaging*. 2024 Jan 2;24(1):2.
4. Katal S, Eibschutz LS, Saboury B, Gholamrezanezhad A, Alavi A. Advantages and Applications of Total-Body PET Scanning. *DX* 2022, 12, 426.

5. Zhang H, Zhang Z, Wang X, Wang D, Xu H, Liu Z, et al. Preparation of trastuzumab-DM1 conjugate with a high drug-to-antibody ratio for breast cancer therapy. *Nano Today*. 2024 Feb 1; 54:102134.
6. Ahad A, Aftab F, Michel A, Lewis JS, Contel M. Development of immunoliposomes containing cytotoxic gold payloads against HER2-positive breast cancers. *RSC med chem*. 2024;15(1):139-50.
7. Shahhosseini S. PET radiopharmaceuticals. *IJPR*. 2011;10(1):1-2.
8. Mohammadpour-Ghazi F, Yousefnia H, Divband G, Zolghadri S, Alirezapour B, Shakeri F. Development and evaluation of  $^{89}\text{Zr}$ -trastuzumab for clinical applications. *AOJNMB*. 2023;11(2):135.
9. Stabin MG, Tagesson M, Thomas SR, Ljungberg M, Strand SE. Radiation dosimetry in nuclear medicine. *Appl Radiat Isot*. 1999 Jan 1;50(1):73-87.
10. Yousefnia H, Zolghadri S, Jalilian AR. Preliminary Dosimetry Study of  $^{67}\text{Ga}$ -AATS for Human Based on Biodistribution Data in Rats. *Iran J Med Phys*. 2015 Jun 1;12(2):121-8.
11. Boodaghi Malidarre R, Khabaz R, Benam MR, Zanganeh V. A feasibility study to reduce the contamination of photoneutrons and photons in organs/tissues during radiotherapy. *Iran J Med Phys*. 2020 Nov 1;17(6):366-73.
12. Sina S, Naderi SM, Karimipourfard M, Molaeimanesh Z, Sadeghi M, Zamani E, et al. Development of a simple method for determining the absorbed activity concentration by the thyroid gland of nuclear medicine staff. *Iran J Med Phys*. 2021 May 1;18:211-7.
13. Stabin MG, Siegel JA. Physical models and dose factors for use in internal dose assessment. *HPHY*. 2003 Sep 1;85(3):294-310.
14. Sparks RB, Aydogan B. Comparison of the effectiveness of some common animal data scaling techniques in estimating human radiation dose. Oak Ridge Associated Universities, TN (United States); 1999 Jan 1.
15. Mohammadpour-Ghazi F, Yousefnia H, Zolghadri S, Yarmohammadi M, Alirezapour B, Rahiminejad A, et al. Production of radioimmunoPET grade zirconium-89. *Iran J Nucl Med*. 2023;31(1):20.
16. Currie LA. Quantifying uncertainty in nuclear analytical measurements. IAEA. Sept 2004 July 1.
17. Bolourinovin F, Mirzaei M, Faghihi R, Joharidaha F, Sina S, Hadad K, Badipa F, Yousefnia H. Preparation, quality control, biodistribution of [ $^{113}\text{mIn}$ ]In-DOTATATE. *J Nuclear Sci Eng Technol*. 2024; 45(3):29-35.
18. Akbari L, Zolghadri S, Karimian A, Yousefnia H, Ranjbar S. Human absorbed dose estimation of [ $^{113}\text{mIn}$ ] In-PSMA-617 for prostate cancer imaging using animal data and Monte Carlo simulation. *J Biomed Phys Eng*. 2025 Aug; 20:1-0.
19. Yousefnia H, Zolghadri S, Jalilian AR, Tajik M, Ghannadi-Maragheh M. Preliminary dosimetric evaluation of  $^{166}\text{Ho}$ -TTHMP for human based on biodistribution data in rats. *Appl Radiat Isot*. 2014 Dec 1; 94:260-5.
20. Stabin MG, Sparks RB, Crowe E. OLINDA/EXM: the second-generation personal computer software for internal dose assessment in nuclear medicine. *J Nucl Med*. 2005 Jun 1;46(6):1023-7.
21. O'Donoghue JA, Lewis JS, Pandit-Taskar N, Fleming SE, Schöder H, Larson SM, et al. Pharmacokinetics, biodistribution, and radiation dosimetry for  $^{89}\text{Zr}$ -trastuzumab in patients with esophagogastric cancer. *J Nucl Med*. 2018 Jan 1;59(1):161-6.
22. Laforest R, Lapi SE, Oyama R, Bose R, Tabchy A, Marquez-Nostra BV, et al. [ $^{89}\text{Zr}$ ] Trastuzumab: evaluation of radiation dosimetry, safety, and optimal imaging parameters in women with HER2-positive breast cancer. *MIBI*. 2016 Dec; 18:952-9.
23. Shanehsazzadeh S, Yousefnia H, Lahooti A, Zolghadri S, Jalilian AR, Afarideh H. Assessment of human effective absorbed dose of  $^{67}\text{Ga}$ -ECC based on biodistribution rat data. *Ann Nucl Med*. 2015 Feb; 29:118-24.
24. Radiological protection in biomedical research, ICRP Publication 62 (1992).
25. Zolghadri S, Mohammadpour-Ghazi F, Yousefnia H. Preclinical studies and absorbed dose estimation of [ $^{89}\text{Zr}$ ]Zr-DFO-Bevacizumab for PET imaging of VEGF-expressing tumors. *Appl Radiat Isot*. 2024 May; 28:111379.
26. Zolghadri S, Mohammadpour-Ghazi F, Yousefnia H. Preparation, quality control, and absorbed dose estimation of  $^{89}\text{Zr}$ -DFO-Cetuximab for imaging of EGFR-expressing tumors. *J Radioanal Nucl Chem*. 2024 Apr; 26:1-0.